

Enhanced White Blood Cell and Platelet Segmentation: A Particle Swarm Optimization-based Chromaticity approach

Aiswarya Senthilvel*, Krishnaveni Marimuthu and Subashini Parthasarathy

Centre for Machine Learning and Intelligence, Department of Computer Science, Avinashilingam Institute for Home Science and Higher Education for Women, Coimbatore, India

ABSTRACT

Microscopic image examination is essential for medical diagnostics to identify anomalies using cell counts based on morphology. Sick Cell Disease (SCD) is an inherited blood condition characterized by defective hemoglobin, leading to severe anemia and complications. Detecting sickle cells in blood smears is essential, but the presence of White blood cells (WBCs) and platelets often leads to miscounting as they are classified incorrectly as red blood cells (RBCs). This study proposed an approach for segmenting WBCs and platelets by resembling the human color recognition process to differentiate the regions for accurate identification. First, the RGB color space is converted to RG chromaticity to locate WBCs and platelets with high pixel chromatic variance. Parametric segmentation is applied to the RG chromaticity images to identify the appropriate chromaticity channel for segmentation based on probability distribution values. The optimal threshold values have been determined using Particle Swarm Optimization (PSO) by dynamically narrowing the search space using values obtained through manual experimentation ranging from 0.001 to 1. This systematic process effectively identifies and segments platelets and WBCs, ensuring that overlapping platelets and WBCs are accurately segmented. Compared to state-of-the-art techniques, the proposed approach achieved an accuracy of 96.32 %, 96.97% for sensitivity, 96.96 % for precision and 97.46% for F- score in the pixel-wise segmentation of WBCs and platelets.

Keywords: Chromaticity, parametric segmentation, particle swarm optimization, platelets, sickle cell disease, white blood cells

ARTICLE INFO

Article history:

Received: 18 November 2024

Accepted: 03 March 2025

Published: 23 April 2025

DOI: <https://doi.org/10.47836/pjst.33.3.24>

E-mail addresses:

21phesf007@avinuty.ac.in (Aiswarya Senthilvel)

krishnaveni_cs@avinuty.ac.in (Krishnaveni Marimuthu)

subashini_cs@avinuty.ac.in (Subashini Parthasarathy)

*Corresponding author

INTRODUCTION

Sickle cell disease (SCD) is an inherited blood disorder characterized by abnormal hemoglobin. This arises when the two aberrant genes are inherited from both parents, leading to the synthesis of

hemoglobin S, which is mainly in charge of the development of irregular red blood cells (RBCs). These abnormal RBCs have difficulty carrying oxygen and get stuck in blood arteries, which can result in many problems, including organ damage, infections, and pain. Because of the significant frequency and serious health effects of hemoglobinopathies worldwide, SCD detection and diagnosis are essential (Alzubaidi, Fadhel, Al-Shamma et al., 2020). SCD national incidence rate was stable between 2000 and 2021; however, the number of newborns with SCD has risen by 13.7% globally due to population growth in the Caribbean, western, and central sub-Saharan Africa. In 2021, the number of patients with SCD increased by 41.4% worldwide. India accounts for 14.5% of infants born with SCD, approximately 42,000 per year, ranking second after sub-Saharan Africa. The quality of life of an individual with SCD can be improved through early diagnosis for disease management. Hematologists examine blood samples under a microscope for diagnosis; this is a time-consuming approach that is subject to errors caused by humans (WHO, 2011). Manual blood smear analysis becomes more difficult due to a difference in cell sizes, shapes, boundaries, and placements, which also challenges screening for the disease. Recent advances in Artificial Intelligence and Machine Learning (ML) have increased recognition and accuracy for diagnosis. Automated equipment assists pathologists and medical professionals in accurately identifying anemia (Acharya & Prakasha, 2019).

Conventional Methods for SCD Identification

SCD has been classified and segmented using different image processing and machine learning techniques (Das et al., 2019). The Circular Hough Transform (CHT) has been used to differentiate between sickle cells and normal RBCs. A fuzzy inference system (FIS) was used together with CHT to differentiate cells and extract the red component. Cell identification and counting have been determined using morphological descriptors, form factors, and gradient-based watershed transformations. Parvathy et al. (2016) analyzed compactness and shape using Otsu's technique and watershed segmentation. Sharma et al. (2016) used marker-controlled watershed transformations to distinguish erythrocytes and K-nearest neighbors (KNN) for classification, whereas Acharya and Kumar (2017) used the K-Medoids approach for erythrocytes segmentation and classification. Neural networks were used by Elsalamony (2017) to classify anemia and Chy and Rahaman (2018) trained a Support Vector Machine (SVM) with several indicators for SCD classification. Many classification methods, such as SVM, Extreme Learning Machine (ELM), and KNN classifiers have been used to distinguish and categorize sickle cells and normal cells (Chy & Rahaman, 2019). Existing approaches concentrate on normal and sickle cell categorization and do not consider the presence of WBCs and platelets in blood smear images. WBCs can be misclassified as RBCs, whereas clustered platelets are often confused with sickle cells. Therefore, enhanced WBC and platelet extraction techniques are necessary to provide an accurate diagnosis.

Deep Learning Methods for SCD Segmentation

Deep learning (DL) methods, such as Recurrent Neural Networks (RNNs) and Deep CNNs, are efficient in medical image data classification (Ker et al., 2017). Convolutional Neural Networks (CNNs) have achieved 86.34% and 87.50% accuracy in RBCs classification (Alzubaidi, Al-Shamma et al., 2020; Xu et al., 2017). DL models require large training datasets to obtain optimal results. Khalaf et al. (2017) used three RNN architectures, whereas Zhang et al. (2018) used a U-Net technique for RBC segmentation. The pre-trained InceptionV3 model extracted 2048 deep features for sickle cell identification (Alagu et al., 2023). An enhanced wrapper-based feature selection approach employing multi-objective binary grey wolf optimization (MO-BGWO), KNN, and SVM was utilized to classify features. The SVM classifier achieved 96% accuracy, which increases system performance. Deep learning techniques depend on well-chosen models and are affected by cell size, color, and form differences. Recent developments in deep learning have shown its potential to address these issues by accurately differentiating normal and sickle-shaped cells based on their features. However, these techniques have difficulty counting sickle and healthy erythrocytes because the present studies do not focus on removing platelets and WBCs from sickle blood smear images, which is essential for cell counting. Deep learning needs the annotation images for the segmentation model, but the dataset does not contain the annotation images. Therefore, the WBCs and platelets for automatic segmentation need to be annotated using a DL-based model for the enhanced process.

Conventional Methods for WBC and Platelets Segmentation

In medical image processing, identifying WBCs is an important area of study. Several researchers have investigated and developed methodologies that leverage deep-learning models and image-processing algorithms to improve WBC detection and classification (Alzubaidi, Fadhel, Oleiwi et al., 2020). WBC segmentation has been studied using several approaches, each with its merits and cons. Certain methods concentrate on segmenting the nucleus or cell (Tosta et al., 2015); however, other methods consider segmenting the nucleus and cytoplasm (Sarrafzadeh & Dehnavi, 2015). Threshold-based segmentation remains one of the easiest and most popular approaches, whether alone or in combination with other strategies. Makem and Tiedeu (2020) employed HSV and CMYK color space color components fused for WBC nuclei identification using adaptive fusion based on principal component analysis. (HSV and CMYK color space color components fused for WBC nuclei detection using adaptive fusion based on principal component analysis. Garcia-Lamont et al. (2021) proposed a method for segmenting WBC nuclei using high chromatic variation in hue components and classifying the cells using unsupervised neural networks. WBC is segmented based on human color discrimination through principal component analysis in HSV, RGB, and $L^*a^*b^*$ spaces which contain chromatic variation by hue extraction without complex mathematical computations (García-Lamont et al., 2022).

Clustering-based segmentation is used to extract WBCs from microscopic images. Tavakoli et al. (2021) proposed a method for segmenting nuclei that combines a balanced color technique with Otsu's thresholding algorithm. The convex hull of the nucleus was then used to detect the cytoplasm, and the SVM was used for classification. Kaur et al. (2016) developed an automated platelet counting method that employs the CHT on microscopic blood images. Their approach was based on platelet size and shape properties, resulting in a 96% accuracy. Cruz et al. (2017) proposed an image analysis framework for segmenting and counting the complete blood count (CBC). Their approach achieved more than 90% accuracy by combining HSV thresholding, linked component identification, and statistical analysis of microscopic blood images. Traditional approaches fail to achieve adequate results due to their variable lighting conditions. State-of-the-art approaches predominantly concentrate on segmenting WBCs and platelets separately rather than combining them in the same study. Traditional processes have limitations and highlight the requirement for improved methodologies to address such challenges with superior precision. Therefore, an individual approach for segmenting WBCs and platelets from blood smear images is essential for improving the precision and effectiveness of medical image analysis.

Deep Learning-based Methods for WBC and Platelets Segmentation

Deep learning (DL) based segmentation can be classified into instance and semantic segments. Instance segmentation detects individual cells, whereas semantic segmentation uses an identical mask for each region of interest (ROI) in a single image to differentiate objects based on pixel-level categorization. The most commonly used network for classifying and segmenting images is CNN. It uses a deep CNN with multiple variables trained on a larger dataset to obtain effective outcomes with deep learning models. Deep learning models are difficult to train on medical datasets because of limited data size; therefore, pretrained models are often used to overcome this limitation. Khouani et al. (2020) utilized various CNN architectures for segmenting WBC, including VGG-16, VGG-19, ResNet-50, ResNet-101, and Inception-v3. ResNet-50, optimized with the Adam optimizer, achieved the highest test accuracy of 95.73%. CNN and pre-trained CNN models are utilized to classify and segment WBCs and platelets process (Anand et al., 2024; Ozcan et al., 2024; Saidani et al., 2024). Ground-truth annotations are essential for the accurate and complete evaluation of deep-learning-based segmentation techniques. Thus, the assessment is based on how precisely and effectively the model identifies regions of interest in medical images. However, the SCD dataset does not contain annotations for WBCs and platelets, making deep learning for segmentation inadequate for this application. This study introduces a method for obtaining accurate ground-truth annotations of WBCs and platelets, which enables effective analysis to assist the segmentation process.

Optimization-based Approaches for Medical Image Segmentation

Optimization-based techniques have gained significant attention for enhancing medical-image segmentation (Wang et al., 2021; Farshi et al., 2020). These methods aim to optimize and fine-tune the segmentation algorithms (Shang et al., 2020). Optimization techniques increase the accuracy and efficiency of segmentation algorithms (Shi et al., 2023; Khosla & Verma, 2023). Existing studies examine classical optimization, metaheuristics, and machine learning-based techniques (Narayana et al., 2022; de Albuquerque et al., 2020; Shehab et al., 2020) with a focus on parameter modifications to minimize segmentation issues and enhance overall performance. PSO is a swarm intelligence-inspired optimization approach widely used in image analysis (Zhang & Lim, 2020; Mandave & Patil, 2023). PSO is effective at addressing complicated, multidimensional problems (Eisham et al., 2023) and is used for feature selection (Kavitha & Chellamuthu, 2019), image registration (Sarvamangala & Kulkarni, 2019), segmentation (Kate & Shukla, 2020; Chakraborty et al., 2019), classification (Singh et al., 2025) and object tracking (Öztürk et al., 2020). PSO effectively examines search regions while reducing local optima, making it a great selection for image analysis. PSO enhances medical image segmentation by determining optimal image segments based on global and local features (Vijh et al., 2020; Shehanaz et al., 2021). The versatility and ability of PSO to solve issues make it an excellent tool for image-processing researchers (Nayak et al., 2023; Dhal et al., 2019). The study proposed by de Albuquerque et al. (2020) expanded the significance of PSO to medical image segmentation by employing its ability to navigate complicated search areas. PSO is well suited for dealing with medical imaging difficulties such as noise, uneven lighting, and complex structures (Guo et al., 2023).

The proposed study uses PSO to improve the accuracy of medical image segmentation, primarily for WBCs and platelets in blood smear images. The study improves segmentation by combining PSO and color space approaches. The contributions of this study are as follows:

- Identification of a suitable color space for WBCs and platelets segmentation in peripheral smear images
- WBCs and platelets were methodically detected using the RG chromaticity approach, with target regions distinguished using parametric segmentation
- Determine the best chromaticity channels for WBC and platelet identification by conducting a comparative examination of the channels
- Particle Swarm Optimization (PSO) was used to construct probability distribution values and optimize the search space for segmentation
- Accuracy of 96.32% on the erythrocyteIDB dataset, demonstrating the efficient results for segmentation

MATERIAL AND METHOD

The proposed approach segmented the platelets and WBCs by combining PSO with image chromaticity. It determined a significant color space, identified regions similar to those of WBCs and platelets, selected the optimal chromaticity channel for segmentation, and applied PSO-based threshold optimization. Figure 1 shows the entire process of segmenting WBCs and platelets.

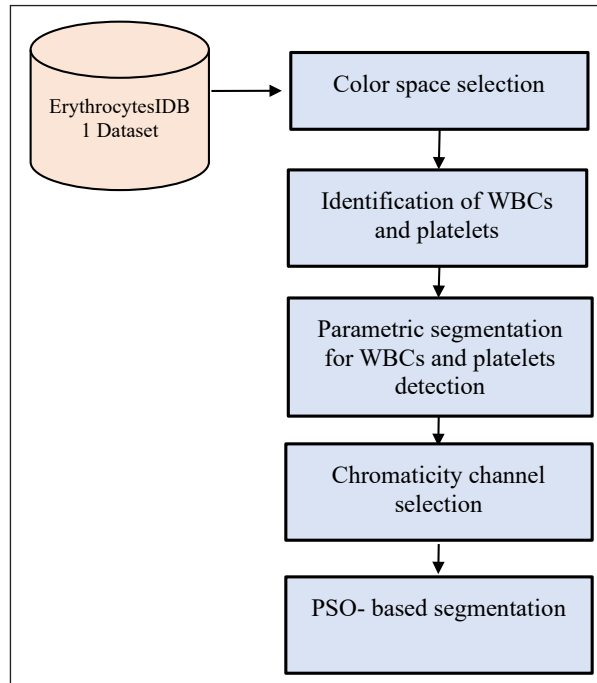


Figure 1. Overview of the Proposed PSO-based segmentation approach for WBCs and platelets segmentation

Identification of Suitable Color Space for WBC and Platelets Detection

This study employed the ErythrocytesIDB1 dataset for a comprehensive analysis. The color space of an image is primarily selected for the segmentation of WBC and platelets. This has different chromatic properties from RBCs. However, selecting the appropriate color space is essential to reduce the influence of the color space for WBC and platelet identification. Blood smear images have color variations because of the staining, lighting conditions, and external characteristics (Fitri et al., 2017). The images were reduced to $256 * 256$ to standardize the image analysis and the color range was normalized using the min-max method (Juliet et al., 2015; Patro et al., 2015). Noise in the images was eliminated using a nonlocal mean (NLM) filter which was selected for its ability to reduce Gaussian noise (Buades et al., 2005). Based on the literature, RGB, HSV, and Lab color spaces were

employed to identify and segment WBCs and platelets. Hue saturation value (HSV) and Lab color spaces are often used for image analysis; however, RGB (red, green, and blue) is still widely used in digital images because of its correspondence with human perception. Figure 2 shows an image of the different color spaces affecting blood cells.

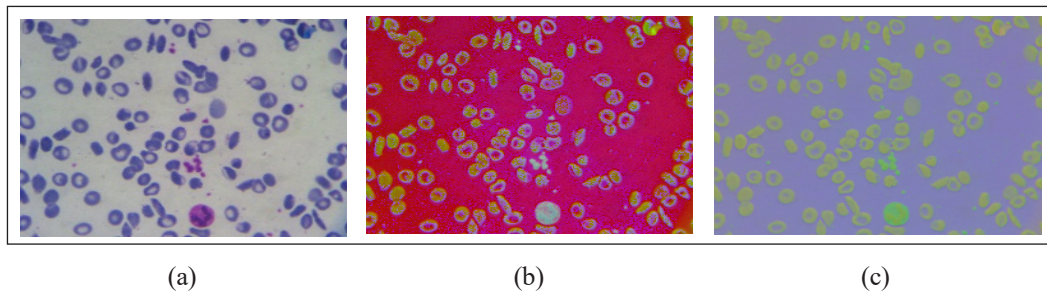


Figure 2. Image representation in different color spaces. (a) RGB color space image; (b) HSV color space image; (c) Lab color space image

WBCs and platelets differ in staining characteristics from RBCs, and it was used to differentiate between them. WBCs typically have a pink to purple color because of their nuclei while platelets are smaller with purple color due to the cytoplasmic granules (Imron & Fitri, 2019). Purple staining in the smear images differentiates WBCs and platelets in RGB color space 2(a), enabling accurate identification across numerous areas. WBCs and platelets are difficult to identify in HSV color space 2(b) because the color regions are not easily distinguished from the human eye. This limitation affects the identification of sickle cells because it affects RBC texture. Similarly, identification is difficult in Lab color space 2(c) because of the distortion of the background hues. The proposed technique uses the RGB color space to identify platelets and WBCs in smear images by maintaining the shapes and textures of the RBCs.

Identification of WBCs and Palettes from Blood Smear Images

Ground truth annotations are required for segmentation tasks to accurately identify regions. However, labeled data are unavailable in this study; therefore, WBC and platelet areas need to be identified prior to segmentation. The RGB color space was selected for such purposes because it is well suited for discriminating between those regions; however, there are limitations in the representation of luminance and brightness, which affects the analysis. This limitation was addressed by converting the RGB color space into a chromaticity format. These chromatic characteristics were separated from the intensity, mimicking human analysis. This is because chromaticity is independent of intensity, as demonstrated by the CIE 1931 xy chromaticity diagram (Sharma, 2017) that converts colors into 2D chromatic coordinates. Luminance-normalized images were determined by normalizing the RGB value to provide (x, y) coordinates on the chromaticity diagram,

representing decreasing brightness. The red (r) and green (g) channels are normalized for RG chromaticity conversion using Equations 1, 2, and 3.

$$r = \frac{R}{(R + G + B)} \quad [1]$$

$$g = \frac{G}{(R + G + B)} \quad [2]$$

$$R + G + B = 1 \quad [3]$$

The normalized red chromaticity component r removes the impact of brightness, whereas the normalized green chromaticity component g provides color as a relative proportion rather than an absolute intensity. Equation 3 sums R , G , and B as the overall intensity, reducing by removing illumination variations, enabling r and g to accurately express chromaticity and minimize dimensionality while maintaining the critical aspects of color (r and g). RG chromaticity separates chromaticity information, which improves color analysis and visual perception, allowing for the better identification of WBCs and platelets. Figure 3 shows the chromaticity distribution of an image, where the source image and chromaticity diagram of the source images are displayed in 3(a) and 3(b), and

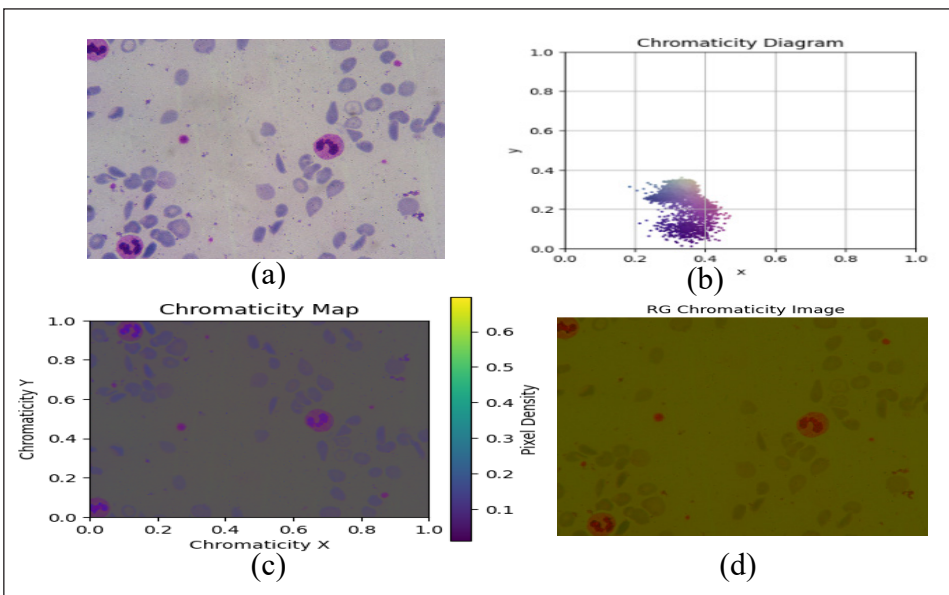


Figure 3. Chromaticity distribution and mapping of an image: (a) WBC and platelets highlighted in pink to purple color in RGB color space; (b) Chromaticity of RGB color space; (c) Chromaticity map of RGB color space; (d) RG chromaticity map

the chromaticity map and RG chromaticity image are shown in 3(c) and 3(d), respectively. Algorithm 1 entails finding the target regions based on the RG Chromaticity pixel density distribution. The RG chromaticity diagram provides significant chromatic variation in WBCs and platelets, which enables accurate differentiation.

Parametric Segmentation Approach for WBC and Platelets Segmentation

This study identified and segmented WBCs and platelets from blood smear images using a parametric segmentation technique (Zhou & Liao, 2022). Because intensity-based thresholding approaches are extensively used for segmentation, the proposed methodology is based on chromatic characteristics. Therefore, standard threshold values are not particularly beneficial. The PS approach divides target areas into a binary mask by utilizing the optimal distribution value. Determining an appropriate threshold value is difficult since different distribution values could provide a binary mask separating foreground and background areas. The PS approach uses a Gaussian distribution to detect WBCs and platelets from RG chromaticity images by concentrating on the region of interest where pixels show a significant degree of chromatic variation.

Algorithm 1: Identification of WBCs and platelets using RG chromaticity

```

Input: rgb_image
(height, width, channels) = image_shape(rgb_image)
r_chromaticity [height, width]
g_chromaticity [height, width]
Chromaticity_map [height, width]
for y from 0 to height - 1
  For x from 0 to width - 1, as follows:
    (R, G, B) = rgb_values (rgb_image, y, x)
    sum = R + G + B
    r = R/sum
    g = G/sum
    r_chromaticity [y, x] = r
    g_chromaticity [y, x] = g
    rg_value = r + g
    chromaticity_map [y, x] =rg value
return
Output: chromaticity_map

```

The statistical parameters mean (μ) and standard deviation (σ) were used to calculate the pixel chromatic variance values to identify the target region. This indicates the average and variance of pixels scattered in a Gaussian distribution. These statistical characteristics, which include μ and σ , are explained by Equations 4, 5, and 6. The Gaussian distribution applied for segmentation is illustrated in Equation 7, which also explains how the correlations between the R and G chromaticity channels at each pixel determine which

colors combine. The equation is applied to the RG, R, and G chromaticity channels to identify which chromaticity channels are associated with WBCs and platelets.

$$\mu = \frac{1}{N} \sum_{c=1}^N p_c \quad [4]$$

$$\sigma^2 = \frac{1}{N} \sum_{c=1}^N (p_c - \mu)^2 \quad [5]$$

$$\sigma = \sqrt{\sigma^2} \quad [6]$$

The mean pixel intensity μ and the variation around the mean define the variance σ^2 and standard deviation σ of the target patches. The variance σ^2 pixel intensities indicate the distribution of values within the target region. Each pixel-intensity p_c inside the patches includes all pixels in image N.

$$P(c) = \frac{1}{\sigma\sqrt{2\pi}} \exp\left(-\frac{(c - \mu)^2}{2\sigma^2}\right) \quad [7]$$

The Gaussian distribution indicating the probability of the intensity $P(c)$ corresponds to the WBCs and platelet color ranges. The Gaussian function's variable c indicates the intensity of a pixel at specific positions within the image. Probabilistic distribution values for RG chromaticity, as well as individual R and G chromaticity channels, were calculated to determine which chromaticity channel was most suitable for the segmentation process. Determining a significant chromaticity channel for WBC and platelet segmentation is difficult because of the variance in illumination and staining of the image. These differences make it difficult and time-consuming to accurately determine the optimal threshold value for segmentation. Furthermore, the high pixel levels of WBCs, platelets, and size made it difficult to manually determine the binary masking values. An extensive manual evaluation selected distribution values ranging from 0.001 to 1. It accurately recognizes WBCs and platelets while providing no false positives by not detecting RBCs. However, the variations in lighting and illumination connected to the images make it difficult to determine an optimal threshold for every image. Therefore, optimization is required to identify the optimal thresholds for the various images. Algorithm 2 provides a complex approach that determines the best chromaticity channel and enables improved WBC and platelet segmentation, subject to imaging scenarios.

Algorithm 2: Identification of Optimal chromaticity channel for segmentation using Parametric segmentation approach

Input: RG chromaticity image

1. Compute μ , σ^2 and σ using Equations 4, 5 and 6

2. Create a probability map using Equation 7

3. Apply a threshold to identify target region:

Threshold = probability map > Threshold

for each channel (RG, R, G):

Calculate μ , σ^2 , σ and probability map

Apply a threshold to identify areas with the desired color range

End

Output: Best chromaticity channel for segmentation**PSO-based WBCs and Platelets Segmentation**

The optimal threshold was determined using the Particle Swarm Optimization (PSO) (Kennedy & Eberhart, 1995). It adequately searches the parameter space using a swarm of particles implemented with values from manual segmentation and thresholds ranging from 0.001 to 1. The threshold values are iteratively modified by analyzing the search space and optimizing their distribution by altering the position and velocity. The position of each particle shows the threshold values and the aim is to determine a set of ideal threshold values that increases the segmentation accuracy. With a population size of 100, each particle represents a candidate solution determined by its personal best position, $pbest$; the global best position, $gbest$; and a stochastic component indicated by two equally distributed factors, φ_1 and φ_2 . Equation 8 demonstrates the updates in position and velocity. In this equation, $v_i(t)$ indicates the velocity of particle i at time t and $x_i(t)$ is the location of the particle. The inertia weight ω (0.729) determines the prior velocity's contribution to the current update, whereas C_1 and C_2 (1.4944) are cognitive and social factors, respectively, directing the particle to its own best and global best places. The random values φ_1 and φ_2 provide variations in the search process, making it more uncertain and allowing a more comprehensive exploration of the solution space. The position update in Equation 9 directs the particle to a new location based on its velocity. The location denotes a potential threshold value, and the velocity controls how much it is altered throughout each iteration.

$$v_i(t + 1) = \omega v_i(t) + C_1 \varphi_1 (pbest(t) - x_i(t)) + C_2 \varphi_2 (gbest(t) - x_i(t)) \quad [8]$$

$$x_i(t + 1) = x_i(t) + v_i(t + 1) \quad [9]$$

The optimization approach was designed to differentiate between the fitness landscape's global optimum and the local extrema. The peak fitness function z in Equation 10 measures

the accurate segmentation of a particle. The function has three exponential elements that address the essential factors that affect the search space. It examines particle locations by calculating a value that indicates the spatial alignment to optimize the threshold value.

$$z = 3 \cdot (1 - x)^2 \exp(-x^2 - y + 12 - 10 \left(\frac{x}{5} - x^3 - y^5\right) \exp(-x^2 - y^2) - \frac{1}{3} \exp(-(x + 1)^2 - y^2) \quad [10]$$

The first exponential term uses decay and polynomial functions to identify regions of interest and calculate the threshold value. The second term improves the complexity by considering the interactions between the x and y coordinates, which helps refine the search in more complex areas. The third term addresses the boundary effects in the search space, which increases the reliability of the fitness measure. The output of the peak fitness function accurately identifies the swarm to the optimal areas and modifies the threshold values for improved segmentation performance. Algorithm 3 outlines the process of determining the optimal threshold value using PSO. Finally, by averaging the threshold values across iterations, the particle swarm converges to the optimal feasible set of segmentation accuracy. The optimal threshold values were 0.87, 0.68, 0.91, and 0.74, increasing the segmentation performance by accurately distinguishing white blood cells, platelets, and RBCs.

Algorithm 3: PSO-based threshold value selection process

Initialize particles:
 For each particle i:
 Initialize position x_i and velocity v_i in the search space [0.001, 1]
 Evaluate fitness value $f(x_i)$ using eq (10)
 Set $pbest = x_i$, $pbestFitness = f(x_i)$
 If $f(x_i)$ is better than global best:
 Set $gbest = x_i$, $gbestFitness = f(x_i)$
 Set $\omega = 0.729$, $\varphi_1 = 1.4944$, $\varphi_2 = 1.4944$
 For each particle i:
 Calculate fitness value $f(x_i)$ using Equation 10
 If $f(x_i)$ is better than particle's personal best:
 Update personal best:
 Set $pbest = x_i$, $pbestFitness = f(x_i)$
 If $f(x_i)$ is better than global best:
 Update global best:
 Set $gbest = x_i$, $gbestFitness = f(x_i)$
 For each particle i:
 random numbers $r1$ and $r2$ distributed in [0, 1]
 Update velocity:
 Update position:
 Use the final $gbest$ as the optimized value
Output: Optimal value for detection

RESULTS AND DISCUSSION

The identified and segmented WBCs and platelets were analyzed qualitatively and quantitatively. The analysis employed several quantitative analytic measures, including accuracy, precision, sensitivity, specificity, and F-score.

Dataset Description

Segmentation analysis was performed using sickle cell smear images from the ErythrocytesIDB1 standard database. The blood samples were taken from SCD patients and are available at <https://erythrocytesidb.uib.es/>. The dataset contains labeled samples characterized by cell morphology as circular, elongated, and other cells. The dataset contained 196 full-field images of platelets, WBCs, and RBCs. In particular, seven images were removed from the database due to imperfections, variation in staining and blurring, whereas 189 images were employed in this study.

Identification of WBC and Platelets Using Chromaticity Feature

RGB color space determines the WBC and platelet regions from blood smear images by converting them into RG chromaticity. Each pixel in the RG chromaticity image is examined to identify the most desirable chromaticity channel for the WBCs and platelet regions. The chromaticity distribution in Figure 4 helps to determine the WBCs and platelets for segmentation. Figure 4(a) displays the source image in the RGB color space, while Figure 4(b) shows RG chromaticity density as a Hexbin map. This map is divided into hexagonal bins, and colors indicate the number of pixels. In contrast, the X and Y axes indicate the spatial distributions of red and green chromaticity channels. Higher color density impacts higher color intensity or darkness, whereas lower color sparsity controls higher color illumination or brighter color. This visualization helps recognize color distribution patterns and identify prominent image color regions.

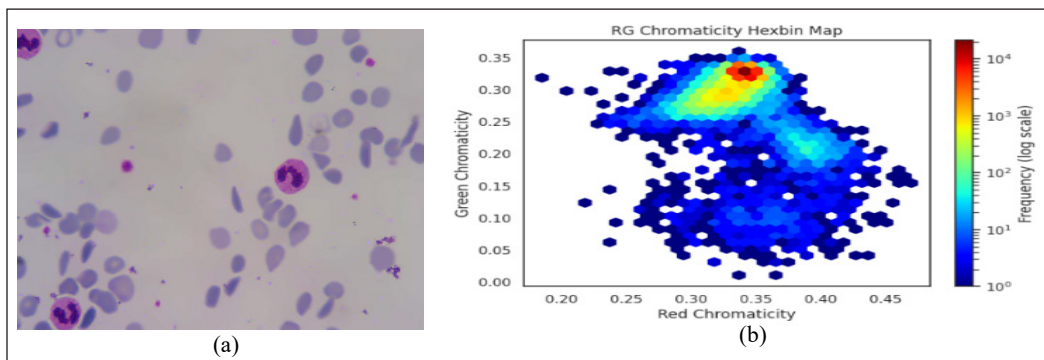


Figure 4. Pixel distribution of RG chromaticity image. (a) Original image; (b) Hexbin representation of RG chromaticity distribution in the smear image

Figure 5 illustrates the density of the pixel distribution in the R and G chromaticity channels for determining WBCs and platelet regions. Figure 5(a) shows the R chromaticity channel with lower pixel density values than the G chromaticity channel in Figure 5(b). The G chromaticity channel exhibited a broader range of pixel density values, extending at both high and low densities. In contrast, the maximum pixel distribution was observed in the G chromaticity channel. The heat map, as shown in Figure 6, provides a graphic representation of the association between red and green components for analyzing each channel of RG chromaticity.

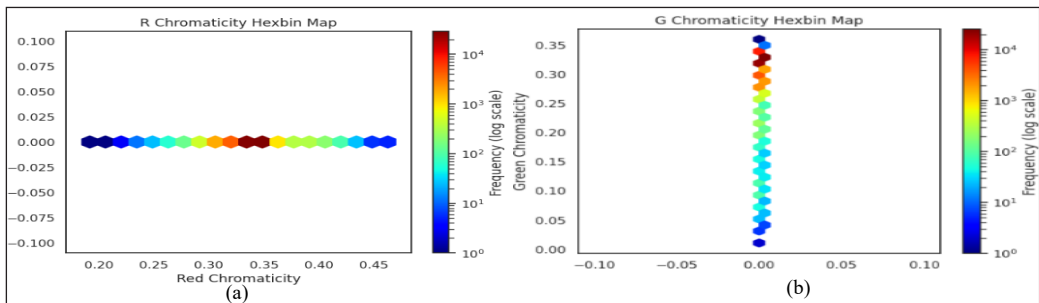


Figure 5. Distribution of chromaticity pixels in the R and G Channels. (a) pixel distribution of R chromaticity channel; (b) pixel distribution of G chromaticity channel

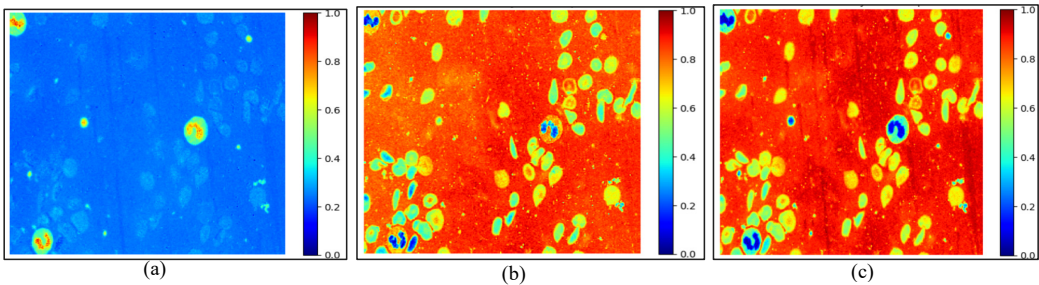


Figure 6. Visualization of RG Chromaticity Heatmap for Target Region Extraction. (a) pixel distribution of RG chromaticity (b) pixel distribution of R chromaticity (c) pixel distribution of G chromaticity

Figure 6(a) shows the RG chromaticity heatmap, while Figures 6(b) and 6(c) display the R and G chromaticity channels, respectively. This examination identified the R and G chromaticity channels as prominent features for identifying WBCs and platelets. These specific areas were retrieved and utilized throughout the segmentation process to identify the target region from the image.

Identification of Optimal Chromaticity Channel for Segmentation

As a result, the WBC and platelets were identified using RG chromaticity, which were considered ground truth images. RG chromaticity and its separate color channels, R and G,

were applied to the parametric segmentation method to identify accurate color channels for segmentation. Figure 7 displays the results, where 7(a) displays the target region retrieved by the chromaticity map. At the same time, 7(b) shows the detection of the regions using RG chromaticity, 7(c) displays the R chromaticity channel that detects WBCs, platelets, and RBC cells, and 7(d) shows the G chromaticity channel, which accurately recognizes the WBCs and platelet regions. The findings demonstrate that RG chromaticity is inefficient for detecting the target regions. In contrast, the R chromaticity channel is limited to the nuclei of WBCs and platelets and detects the RBCs with a bright color.

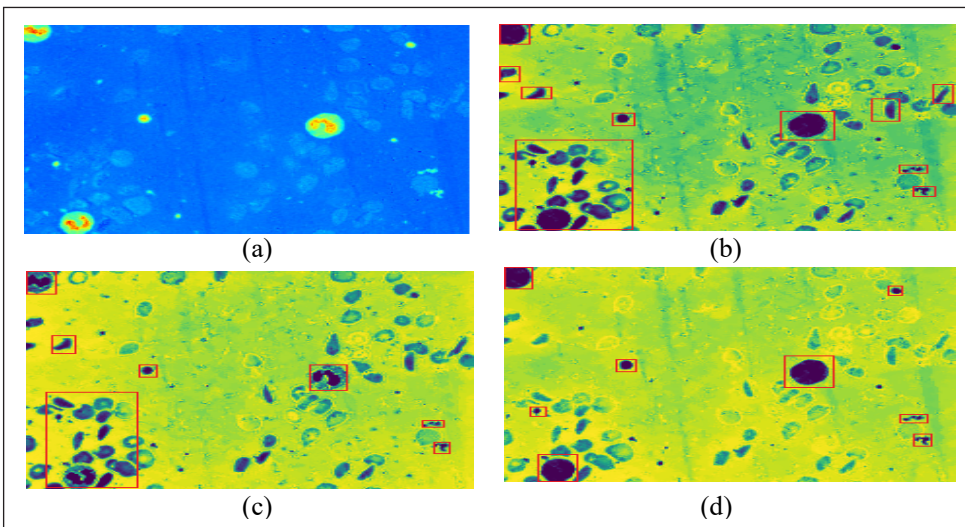


Figure 7. Detection of WBCs and Platelets using RG Chromaticity and separate R and G chromaticity. (a) RG chromaticity map; (b) Parametric segmentation in RG chromaticity; (c) Parametric segmentation in R chromaticity channel; (d) Parametric segmentation in G chromaticity channel

However, the G chromaticity channel highlights WBCs and platelets in the smear image, effectively suppressing other cells by minimizing the impact of illumination and lighting conditions. Based on the examination findings, the G-chromaticity channel was more effective for segmentation.

Identification of Optimal Threshold Value Using PSO

Identifying appropriate threshold values for segmenting WBCs and platelets across various staining images is difficult. Manual segmentation is applied in RG chromaticity and separate R and G channels to determine the appropriate chromaticity channel for WBCs and platelet segmentation. For manual segmentation, the distribution value ranges were selected from 0.001 to 1 and were randomly applied to identify the appropriate channel and visual representation, as shown in Figure 8.

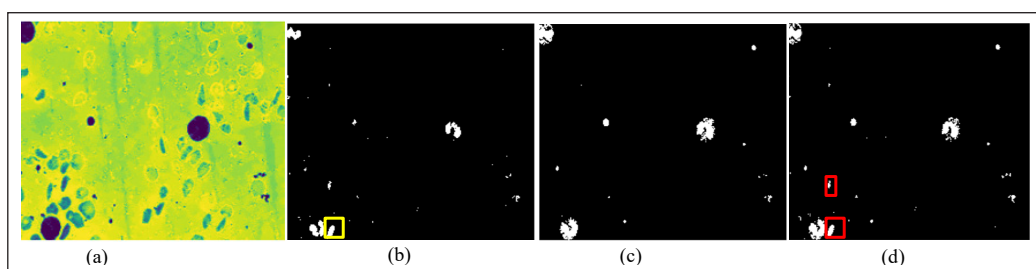


Figure 8. Target region (WBCs and Platelets) binary masked by RG chromaticity and R and G separate channels. (a) Parametric segmentation of WBC and platelets using G chromaticity channel; (b) Target regions detection using R chromaticity channel; (c) Target regions detection using G chromaticity channel; (d) Target regions detection using RG chromaticity channel

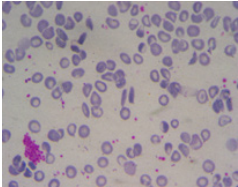


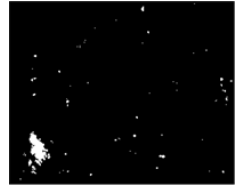
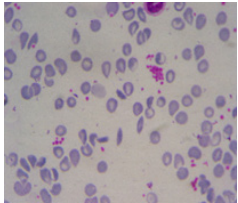

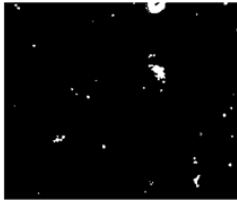
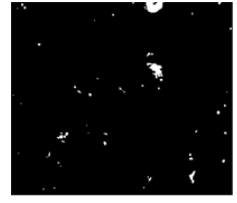
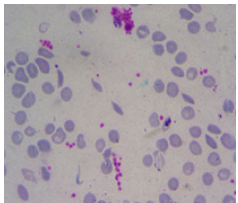
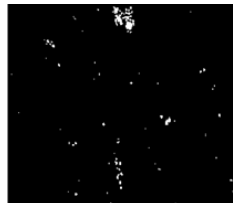

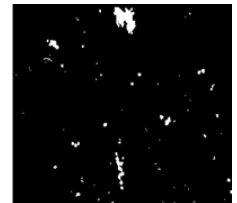
Figure 8 displays the experimental results for determining the RG chromaticity channel for WBCs and platelet segmentation using a manual threshold of 0.01. Figure 8(a) shows the targeted region of the G chromaticity image, whereas the regions segmented by the R, G, and RG chromaticity channels are presented in 8(b), 8(c), and 8(d). The findings show that the R chromaticity channel is highly sensitive to the WBCs nucleus and platelet cells, as shown by the yellow box in 8(b). However, it also identifies the color of RBCs while distinguishing each cell. The G chromaticity channel segments the nucleus and cytoplasm of WBCs and platelets while excluding RBCs alone, as shown in 8(c). The RG chromaticity in 8(d) shows the detection of WBCs and platelets and the presence of certain RBCs enclosed within the highlighted red box. These findings demonstrate that the G chromaticity channel can detect WBCs and platelets in the images. However, the manual method is time-consuming and labor-intensive for finding the appropriate threshold value for segmentation. The experimental results of manual segmentation using RG, R, and G chromaticity are shown in Table 1. The manual threshold value of 0.01 is applied for the segmentation process, which fails the segmentation. This limitation is solved using the PSO algorithm by determining the optimal threshold values of 0.68, 0.74, 0.87 and 0.91.

Accurate detection of WBCs and platelets in smear images was achieved using search space optimization, using the range from 0.001 to 1 probability distribution as a search space in the optimization process with the peak's fitness function. From the optimized search space, the threshold values of 0.68, 0.74, 0.87 and 0.91 were achieved for different staining and illuminated images. The segmentation method successfully segmented the target regions using manual and optimized techniques with the G chromaticity channel. Figure 9 shows the segmentation results with a manual and optimal threshold value of 0.01 and 0.87, respectively.

Figure 9(a) shows the source images, and 9(b) shows the target region identified by the G chromaticity channel. Segmentation of platelets and WBCs using manual and optimized threshold values is shown in 9(c) and 9(d), respectively. The segmentation results in Figure

Table 1

Segmentation of WBC and platelets using RG chromaticity, R and G chromaticity channels with 0.01 threshold value

| Source Image | R Chromaticity Channel | G Chromaticity Channel | RG Chromaticity Channel |
|--|--|--|---|
|  |  |  |  |
|  |  |  |  |
|  |  |  |  |

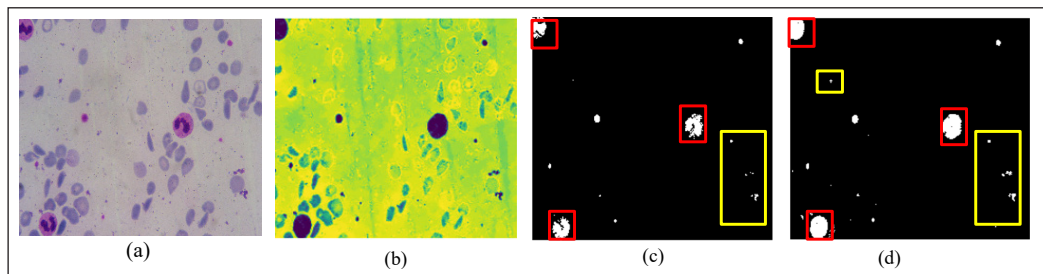


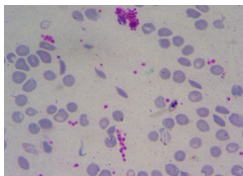
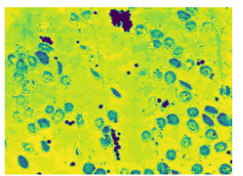


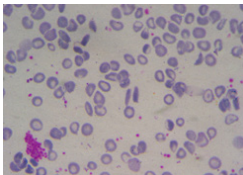
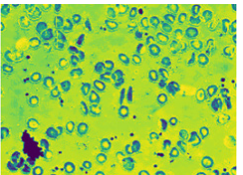


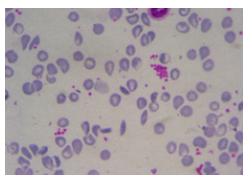
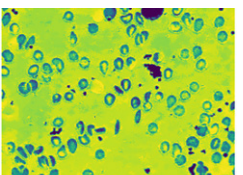


Figure 9. WBC and platelet detection are done using manual and optimal thresholds. (a) Blood smear source image; (b) Parametric segmentation of WBC and platelets using G chromaticity channel; (c) Target region detection using a manual threshold value of 0.01 in G chromaticity channel; (d) Target region detection using an optimized threshold value of 0.87 in G chromaticity channel

9(c) demonstrate that the manual threshold-based technique recognizes only the nuclei of WBCs. In contrast, the cytoplasmic regions are inadequately segmented, as highlighted by the red box. As shown in the yellow box, platelet segmentation was also ineffective for smaller platelets with unclear boundary regions. Figure 9(d) depicts the implementation of an enhanced threshold for segmentation utilizing a Particle Swarm Optimization-based

approach, resulting in significant improvements in results. The red box indicates that both the nucleus and the cytoplasm were detected. The yellow box depicts the optimal threshold value of 0.87, improving the segmentation of small and large platelets over manual thresholding.

The results indicated the significance of selecting accurate threshold values by emphasizing the limitations of manual methods for WBCs and platelet segmentation. The optimization process improved the accuracy and effectiveness of the WBCs and platelet detection approach by segmenting the nucleus and cytoplasm of WBCs and large and small pixels of platelets without including RBCs for the segmentation. It emphasized the significance of the optimized threshold values. The experimental segmentation results using the manual and optimal threshold value are demonstrated in Table 2. The table shows the source images and target regions acquired from the G chromaticity space using manual and optimal threshold values for the segmentation results. Manual segmentation employed 0.01, 0.05, and 0.01 thresholds for each image. In comparison, a PSO-based technique provided optimal thresholds of 0.87 for the first and third images and 0.74 for the second image. Threshold modifications are caused by a variation in lighting conditions between the first and third images, including the second image, which affects the selection of optimal threshold values.

Table 2
Comparison of G chromaticity segmentation using manual and optimal threshold values

| Source Image | G chromaticity space | Segmentation using Manual threshold values | Segmentation using Optimal threshold values from PSO |
|---|---|---|--|
|  |  |  |  |
|  |  |  |  |
|  |  |  |  |

Manual segmentation effectively detects the region of interest and excludes RBCs; however, it has limitations in segmenting small pixel-sized sections and identifying cell borders and edges. The PSO-based technique is superior because it employs optimal threshold values for efficiently segmenting large and small pixel-sized regions without losing their edges, resulting in increased segmentation precision. The segmentation results demonstrate that the PSO approach effectively selects threshold values. This method enables precise segmentation of WBCs and platelets by employing ideal threshold values of 0.68, 0.74, 0.87, and 0.91 for distinct images under diverse lighting and staining conditions.

Quantitative Analysis

In quantitative analysis, pixel-wise binary segmentation is examined by comparing segmented images with their ground truth, which is identified by chromaticity variance and distinctive features of WBCs and platelets in microscopic images (Imron et al., 2019). The quantitative measures used for analysis included accuracy (*Acc*), specificity (*Spe*), sensitivity (*Sen*), precision (*Pre*), and F-score. Here, specificity determines how accurately a background is segmented where RBCs are considered the background; precision measures how accurately the images are segmented by ensuring that background (RBCs) pixels are not incorrectly classified as WBC or platelets. The sensitivity indicates the accuracy of the segmented images by ensuring that WBC and platelet pixels have been correctly recognized and not mistakenly classified as background (RBCs). The computations for these findings are based on Equations 11 to 15. The pixel-wise categorization of True Positives (TP), False Negatives (FN), False Positives (FP), and True Negatives (TN) is summarized in Table 3.

$$Acc = \frac{TP + TN}{TP + TN + FP + FN} \quad [11]$$

$$Spe = \frac{TN}{TN + FP} \quad [12]$$

$$Sen = \frac{TP}{TP + FN} \quad [13]$$

$$Pre = \frac{TP}{TP + FP} \quad [14]$$

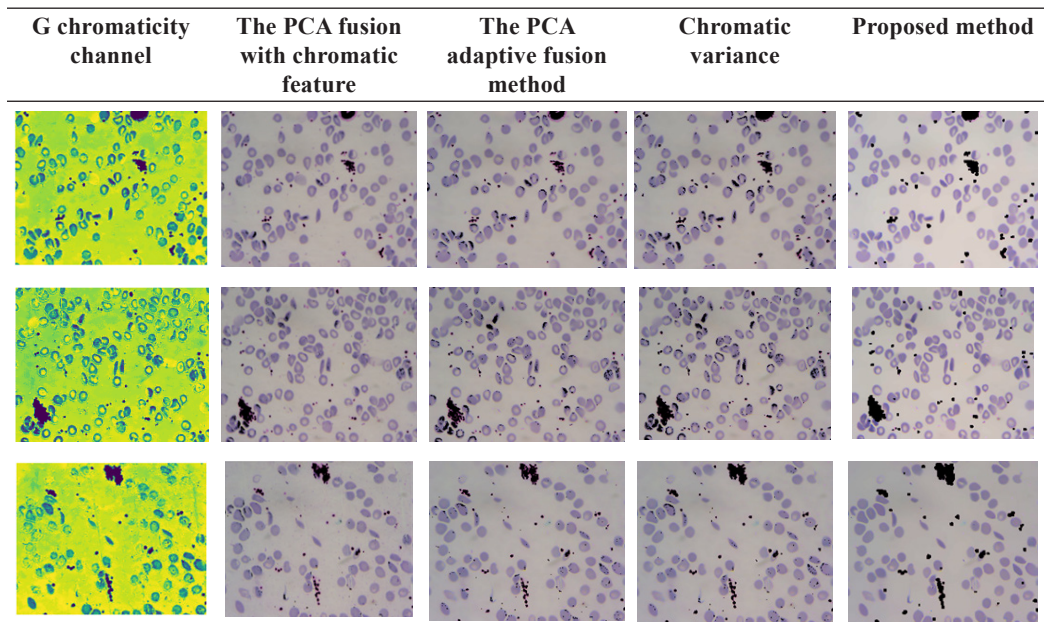
$$F = \frac{2TP}{2TP + FP + FN} \quad [15]$$

Table 3
Classification of WBC and platelets pixel segmentation

| Metrics | Ground truth | Segmented as |
|---------|--------------------|--------------------|
| TP | WBCs and Platelets | WBCs and Platelets |
| FP | Background (RBCs) | WBCs and Platelets |
| TN | Background (RBCs) | Background (RBCs) |
| FN | WBCs and Platelets | Background (RBCs) |

Table 4 presents the state-of-the-art techniques for segmenting WBC and platelets. This comparative study focused on chromatic-feature-based approaches. The PCA-based adaptive fusion of HSV and CMYK (Makem & Tiedeu, 2020) correctly recognizes the nucleus area of WBCs but fails to distinguish the cytoplasm and small platelet pixels. PCA fusion with chromatic features from RGB, HSV, and L*a*b* color space (Garcia-Lamont et al., 2021) accurately detects WBCs and platelets; however, this technique is ineffective for locating the cytoplasm in WBCs. Furthermore, this approach fails to detect the edges of WBCs and platelets, whereas it detects bright pixels of RBCs.

Table 4
Qualitative evaluation comparison of segmented images with state-of-the-art techniques



The chromatic variance approach accurately detected the nuclei and cytoplasm of WBCs and platelets (García-Lamont et al., 2022). However, it has limitations when utilized for sickle cell imaging because it identifies unwanted RBCs with bright regions. Table 5 presents the quantitative analysis findings from the state-of-the-art techniques. The results

Table 5

Quantitative evaluation comparison of segmented images with state-of-the-art techniques

| Method | Accuracy (%) | Precision (%) | Sensitivity (%) | Specificity (%) | F- Score (%) |
|--|---------------------|----------------------|------------------------|------------------------|---------------------|
| The PCA fusion with chromaticity method (Makem & Tiedeu, 2020) | 77.30 | 80.56 | 80.20 | 72.58 | 81.41 |
| The PCA-based adaptive fusion (Garcia-Lamont et al., 2021) | 85.53 | 87.34 | 88.69 | 78.95 | 88.78 |
| Chromatic variance (García-Lamont et al., 2022) | 82.28 | 86.73 | 85.00 | 77.59 | 85.86 |
| Proposed approach with manual method | 92.79 | 95.89 | 93.94 | 83.33 | 95.88 |
| Proposed approach with an optimized method | 96.32 | 96.96 | 96.97 | 94.59 | 97.46 |

demonstrate that the proposed PSO approach has achieved an accuracy of 96.32%. These results show that the proposed method accurately identifies and segments overlapped WBC and platelets from smear images and has significantly improved performance. The analysis demonstrates that the proposed approach is highly efficient for recognizing and detecting WBCs and platelets while excluding RBCs from the segmentation, which resulted in efficiencies of the optimal threshold value. The experimental findings indicate that the proposed method efficiently identifies and segments the WBCs and platelets while excluding RBCs for the segmentation process. The proposed segmentation approach recognizes WBCs and platelets by examining chromaticity components using the advantages of significant pixel variance for accurate identification and differentiation. This method uses RG chromaticity and a parametric approach to determine the probability distribution for accurate segmentation. Variations in staining and lighting conditions can cause a challenge to blood cell segmentation, as shown by the erythrocytesIDB1 dataset. The first 130 images have different staining and lighting conditions than the final 59 images. Even with these variations, the proposed approach effectively responds to changes, and the segmentation accuracy is higher compared to previous studies, as seen in Table 5. Existing research has concentrated on segmenting WBCs into cropped images, which is not suitable for whole-blood-smear images for cell segmentation. State-of-the-art techniques often fail to segment WBCs and platelets because of color illumination and variation problems. WBCs and

platelets are difficult to segment because of size differences and overlapping regions. Most existing approaches fail to segment platelets because they are small and often appear to be small elements in the image. This size differential and platelet overlapping significantly limit the implementation of a single technique for both WBCs and platelets.

Existing chromaticity-based cell segmentation methods have demonstrated various levels of accuracy. PCA fusion based on chromatic attributes from HSV and CMYK color spaces achieved an accuracy of 77.30% because color values varied among the images, impairing RBC region detection. The PCA-based adaptive fusion approach, which utilizes RGB, HSV, and $L^*a^*b^*$ color spaces, obtained an accuracy of 85.53%. This approach accurately recognizes the nucleus but fails to detect very small platelets without separating the hue components from the color space. The chromatic variance approach, which employed the RGB color space, attained an 82.28% accuracy because of its inefficiency in segmenting WBC cytoplasm. The primary limitation of these approaches is their inability to achieve accurate segmentation across datasets with differences in lighting conditions and staining variances. However, the proposed method overcomes this challenge by utilizing RG chromaticity and a Particle Swarm Optimization-based approach to determine the optimal threshold for segmentation with 96.32% accuracy. Despite its limitations, the proposed approach efficiently addresses these challenges and provides precise segmentation.

Furthermore, the proposed method achieved higher accuracy and sensitivity compared to existing methods, because the color component was included as a significant feature and an optimized technique for threshold-value identification. Compared to the traditional manual threshold process, the proposed method improves specificity by systematically optimizing the threshold, resulting in an accurate segmentation of the WBC nucleus and cytoplasm, as well as various-sized pixels of platelets. Based on an artificial intelligence perspective, the proposed approach is bioinspired and reflects how humans observe colors. Recent experiments on CNNs for WBC segmentation were effective; however, they usually required longer processing, but the suggested technique has the lowest computational cost. Moreover, implementing CNNs requires ground truth images for efficient segmentation training. However, the dataset used in this study did not contain ground truth annotations. The proposed method uses RG chromaticity images with parametric segmentation that involves mathematical operations to find the appropriate chromaticity channel for segmentation with a low computational time. The optimal distribution value for segmentation involves the search space optimization with a low computational cost. Therefore, overlapping WBCs and platelets were identified and segmented using the proposed method and are highly computationally competitive. This study has limitations because it focuses on image processing and optimization methodologies rather than implementing CNN-based deep learning models. These models commonly require ground truth annotations during the segmentation phase; however, this dataset fails to provide such annotations. This drawback

can be overcome by employing the segmented images generated by this method as ground truth annotations, allowing the integration of CNN-based segmentation algorithms to achieve more precision and accuracy.

CONCLUSION

Early diagnosis of SCD is essential for effective treatment, with accurate erythrocyte counts being important in both diagnosis and tracking the progression of the disease. Current cell counting methods misidentified WBCs and platelets as RBCs, resulting in inaccurate cell detection and false diagnosis. The proposed method uses high chromatic variance to find WBCs and platelets in blood smear images. This is performed by applying parametric segmentation to RG chromaticity and its separate channels to identify the WBCs and platelets pixels that display the highest contrast to the average color of the other blood smear components. The proposed method uses PSO-based optimization in the search space to identify the best threshold values for accurate segmentation. Moreover, chromaticity has been considered as a feature rather than separating color components through experimentation, which often occurs in state-of-the-art methods. In this experiment, the performance of the segmentation method was examined by comparing the WBCs and platelets using chromatic images as the ground truth. Previous methodologies segmented WBCs and platelets from separate experiments instead of within a single study. In comparison, the proposed method achieved a precision and sensitivity of 96.96% and 96.97%, respectively, with a higher accuracy of 96.32%. In future work, CNNs will be used for automatic WBC and platelet segmentation. The segmented regions will be eliminated to increase the RBC counts for abnormality detection. This automation has the ability to enhance treatments and reduce the emphasis on manual interventions, thereby improving medical diagnosis accuracy and efficiency. This method can identify leukemia by determining the most effective chromaticity channel for improved WBC segmentation for disease identification.

ACKNOWLEDGEMENT

This work is supported by the Centre for Machine Learning and Intelligence (CMLI), which is ISO Certified (ISO/IEC 20000-1:2018) and funded by the Department of Science and Technology (DST-CURIE).

REFERENCES

Acharya, V., & Kumar, P. (2017). Identification and red blood cell classification using computer aided system to diagnose blood disorders. In *2017 International Conference on Advances in Computing, Communications and Informatics (ICACCI)* (pp. 2098-2104). IEEE Publishing. <https://doi.org/10.1109/icacci.2017.8126155>

- Acharya, V., & Prakasha, K. (2019). Computer aided technique to separate the red blood cells, categorize them and diagnose sickle cell anemia. *Journal of Engineering Science & Technology Review*, 12(2), 67-80. <https://doi.org/10.25103/jestr.122.10>
- Alagu, S., Ganesan, K., & Bagan, K. B. (2023). A novel deep learning approach for sickle cell anemia detection in human RBCs using an improved wrapper-based feature selection technique in microscopic blood smear images. *Biomedical Engineering/Biomedizinische Technik*, 68(2), 175-185. <https://doi.org/10.1515/bmt-2021-0127>
- Alzubaidi, L., Al-Shamma, O., Fadhel, M. A., Farhan, L., & Zhang, J. (2020). Classification of red blood cells in sickle cell anemia using deep convolutional neural network. In *Intelligent Systems Design and Applications: 18th International Conference on Intelligent Systems Design and Applications (ISDA 2018)* (pp. 550-559). Springer. https://doi.org/10.1007/978-3-030-16657-1_51
- Alzubaidi, L., Fadhel, M. A., Al-Shamma, O., & Zhang, J. (2020). Robust and efficient approach to diagnose sickle cell anemia in blood. In *Intelligent Systems Design and Applications: 18th International Conference on Intelligent Systems Design and Applications (ISDA 2018)* (pp. 560-570). Springer. https://doi.org/10.1007/978-3-030-16657-1_52
- Alzubaidi, L., Fadhel, M. A., Oleiwi, S. R., Al-Shamma, O., & Zhang, J. (2020). DFU_QUTNet: Diabetic foot ulcer classification using novel deep convolutional neural network. *Multimedia Tools and Applications*, 79(21), 15655-15677. <https://doi.org/10.1007/s11042-019-07820-w>
- Anand, V., Gupta, S., Koundal, D., Alghamdi, W. Y., & Alsharbi, B. M. (2024). Deep learning-based image annotation for leukocyte segmentation and classification of blood cell morphology. *BMC Medical Imaging*, 24(1), Article 83. <https://doi.org/10.1186/s12880-024-01254-z>
- Buades, A., Coll, B., & Morel, J. M. (2005). A non-local algorithm for image denoising. In *2005 IEEE Computer Society Conference on Computer Vision and Pattern Recognition (CVPR'05)* (Vol. 2, pp. 60-65). IEEE Publishing. <https://doi.org/10.1109/cvpr.2005.38>
- Chakraborty, R., Sushil, R., & Garg, M. L. (2019). An improved PSO-based multilevel image segmentation technique using minimum cross-entropy thresholding. *Arabian Journal for Science and Engineering*, 44, 3005-3020. <https://doi.org/10.1007/s13369-018-3400-2>
- Chy, T. S., & Rahaman, M. A. (2018). Automatic sickle cell anemia detection using image processing technique. In *2018 International Conference on Advancement in Electrical and Electronic Engineering (ICAEEE)* (pp. 1-4). IEEE Publishing. <https://doi.org/10.1109/icaeee.2018.8642984>
- Chy, T. S., & Rahaman, M. A. (2019). A comparative analysis by KNN, SVM & ELM classification to detect sickle cell anemia. In *2019 International Conference on Robotics, Electrical and Signal Processing Techniques (ICREST)* (pp. 455-459). IEEE Publishing. <https://doi.org/10.1109/icrest.2019.8644410>
- Cruz, D., Jennifer, C., Castor, L. C., Mendoza, C. M. T., Jay, B. A., Jane, L. S. C., & Brian, P. T. B. (2017). Determination of blood components (WBCs, RBCs, and Platelets) count in microscopic images using image processing and analysis. In *2017 IEEE 9th International Conference on Humanoid, Nanotechnology, Information Technology, Communication and Control, Environment and Management (HNICEM)* (pp. 1-7). IEEE Publishing. <https://doi.org/10.1109/hnicem.2017.8269515>

- Das, P. K., Meher, S., Panda, R., & Abraham, A. (2019). A review of automated methods for the detection of sickle cell disease. *IEEE Reviews in Biomedical Engineering*, *13*, 309-324. <https://doi.org/10.1109/RBME.2019.2917780>
- de Albuquerque, V. H. C., Gupta, D., De Falco, I., Sannino, G., & Bouguila, N. (2020). Special issue on bio-inspired optimization techniques for biomedical data analysis: Methods and applications. *Applied Soft Computing*, *95*, Article 106672.
- Dhal, K. G., Ray, S., Das, A., & Das, S. (2019). A survey on nature-inspired optimization algorithms and their application in image enhancement domain. *Archives of Computational Methods in Engineering*, *26*(5), 1607-1638. <http://dx.doi.org/10.1007/s11831-018-9289-9>
- Eisham, Z. K., Haque, M. M., Rahman, M. S., Nishat, M. M., Faisal, F., & Islam, M. R. (2023). Chimp optimization algorithm in multilevel image thresholding and image clustering. *Evolving Systems*, *14*(4), 605-648. <https://doi.org/10.1007/s12530-022-09443-3>
- Elsalamony, H. A. (2017). Anaemia cells detection based on shape signature using neural networks. *Measurement*, *104*, 50-59. <https://doi.org/10.1016/j.measurement.2017.03.012>
- Farshi, T. R., Drake, J. H., & Özcan, E. (2020). A multimodal particle swarm optimization-based approach for image segmentation. *Expert Systems with Applications*, *149*, Article 113233. <https://doi.org/10.1016/j.eswa.2020.113233>
- Fitri, Z. E., Purnama, I. K. E., Pramunanto, E., & Pumomo, M. H. (2017). A comparison of platelets classification from digitalization microscopic peripheral blood smear. In *2017 International Seminar on Intelligent Technology and Its Applications (ISITIA)* (pp. 356-361). IEEE Publishing. <https://doi.org/10.1109/isitia.2017.8124109>
- García-Lamont, F., Alvarado, M., & Cervantes, J. (2021). Systematic segmentation method based on PCA of image hue features for white blood cell counting. *Plos One*, *16*(12), Article e0261857. <https://doi.org/10.1371/journal.pone.0261857>
- García-Lamont, F., Alvarado, M., López-Chau, A., & Cervantes, J. (2022). Efficient nucleus segmentation of white blood cells mimicking the human perception of color. *Color Research & Application*, *47*(3), 657-675. <https://doi.org/10.1002/col.22752>
- Guo, J., Ma, J., García-Fernández, Á. F., Zhang, Y., & Liang, H. (2023). A survey on image enhancement for Low-light images. *Heliyon*, *9*(4), Article e14558. <https://doi.org/10.1016/j.heliyon.2023.e14558>
- Imron, A. M. N., & Fitri, Z. E. (2019). A classification of platelets in peripheral blood smear image as an early detection of myeloproliferative syndrome using gray level co-occurrence matrix. In *Journal of Physics: Conference Series (Vol. 1201, No. 1, p. 012049)*. IOP Publishing. <https://doi.org/10.1088/1742-6596/1201/1/012049>
- Juliet, S., Rajsingh, E. B., & Ezra, K. (2015). Projection-based medical image compression for telemedicine applications. *Journal of Digital Imaging*, *28*, 146-159. <https://doi.org/10.1007/s10278-014-9731-y>
- Kate, V., & Shukla, P. (2020). Image segmentation of breast cancer histopathology images using PSO-based clustering technique. In *Social Networking and Computational Intelligence: Proceedings of SCI-2018* (pp. 207-216). Springer. http://dx.doi.org/10.1007/978-981-15-2071-6_17

- Kaur, P., Sharma, V., & Garg, N. (2016). Platelet count using image processing. In *2016 3rd International Conference on Computing for Sustainable Global Development (INDIACom)* (pp. 2574-2577). IEEE Publishing.
- Kavitha, A. R., & Chellamuthu, C. (2019). Brain tumour detection using self-adaptive learning PSO-based feature selection algorithm in MRI images. *International Journal of Business Intelligence and Data Mining*, *15*(1), 71-97. <http://dx.doi.org/10.1504/IJBIDM.2019.100469>
- Kennedy, J., & Eberhart, R. (1995). Particle swarm optimization. In *Proceedings of ICNN'95-International Conference on Neural Networks (Vol. 4, pp. 1942-1948)*. IEEE Publishing. <https://doi.org/10.1109/ICNN.1995.488968>
- Ker, J., Wang, L., Rao, J., & Lim, T. (2017). Deep learning applications in medical image analysis. *IEEE Access*, *6*, 9375-9389. <https://doi.org/10.1109/access.2017.2788044>
- Khalaf, M., Hussain, A. J., Keight, R., Al-Jumeily, D., Keenan, R., Chalmers, C., Fergus, P., Salih, W., Abd, D. H., & Idowu, I. O. (2017). Recurrent neural network architectures for analysing biomedical data sets. In *2017 10th International Conference on Developments in eSystems Engineering (DeSE)* (pp. 232-237). IEEE Publishing. <https://doi.org/10.1109/dese.2017.12>
- Khosla, T., & Verma, O. P. (2023). Optimal threshold selection for segmentation of Chest X-Ray images using opposition-based swarm-inspired algorithm for diagnosis of pneumonia. *Multimedia Tools and Applications*, *83*(9), 27089-27119. <http://dx.doi.org/10.1007/s11042-023-16494-4>
- Khouani, A., El Habib Daho, M., Mahmoudi, S. A., Chikh, M. A., & Benzineb, B. (2020). Automated recognition of white blood cells using deep learning. *Biomedical Engineering Letters*, *10*, 359-367. <https://doi.org/10.1007/s13534-020-00168-3>
- Makem, M., & Tiedeu, A. (2020). An efficient algorithm for detection of white blood cell nuclei using adaptive three-stage PCA-based fusion. *Informatics in Medicine Unlocked*, *20*, Article 100416. <https://doi.org/10.1016/j.imu.2020.100416>
- Mandave, D. D., & Patil, L. V. (2023). Bio-inspired computing algorithms in dementia diagnosis - A application-oriented review. *Results in Control and Optimization*, *12*, Article 100276. <https://doi.org/10.1016/j.rico.2023.100276>
- Narayana, V. L., Patibandla, R. S. M. L., Pavani, V., & Radhika, P. (2022). Optimized nature-inspired computing algorithms for lung disorder detection. In *Nature-Inspired Intelligent Computing Techniques in Bioinformatics* (pp. 103-118). Springer.
- Nayak, J., Swapnarekha, H., Naik, B., Dhiman, G., & Vimal, S. (2023). 25 years of particle swarm optimization: Flourishing voyage of two decades. *Archives of Computational Methods in Engineering*, *30*(3), 1663-1725. <http://dx.doi.org/10.1007/s11831-022-09849-x>
- Ozcan, S. N., Uyar, T., & Karayegen, G. (2024). Comprehensive data analysis of white blood cells with classification and segmentation by using deep learning approaches. *Cytometry Part A*, *105*(7), 501-520. <https://doi.org/10.1002/cyto.a.24839>
- Öztürk, Ş., Ahmad, R., & Akhtar, N. (2020). Variants of artificial bee colony algorithm and its applications in medical image processing. *Applied Soft Computing*, *97*, Article 106799. <https://doi.org/10.1016/j.asoc.2020.106799>

- Parvathy, H., Hariharan, S., & Aruna, S. (2016). A real-time system for the analysis of sickle cell anemia blood smear images using image processing. *International Journal of Innovative Research in Science, Engineering and Technology*, 5(4), 6200-6207.
- Patro, S. (2015). *Normalization: A preprocessing stage*. *ArXiv Preprint*. <https://doi.org/10.17148/iarjset.2015.2305>
- Saidani, O., Umer, M., Alturki, N., Alshardan, A., Kiran, M., Alsubai, S., Kim, T. H., & Ashraf, I. (2024). White blood cells classification using multi-fold pre-processing and optimized CNN model. *Scientific Reports*, 14(1), Article 3570. <https://doi.org/10.1038/s41598-024-52880-0>
- Sarrafzadeh, O., & Dehnavi, A. M. (2015). Nucleus and cytoplasm segmentation in microscopic images using K-means clustering and region growing. *Advanced Biomedical Research*, 4(1), Article 174. <https://doi.org/10.4103/2277-9175.163998>
- Sarvamangala, D. R., & Kulkarni, R. V. (2019). A comparative study of bio-inspired algorithms for medical image registration. In J. K. Mandal, P. Dutta & S. Mukhopadhyay (Eds.), *Advances in Intelligent Computing* (pp. 27-44). Springer. https://doi.org/10.1007/978-981-10-8974-9_2
- Shang, H., Zhao, S., Du, H., Zhang, J., Xing, W., & Shen, H. (2020). A new solution model for cardiac medical image segmentation. *Journal of Thoracic Disease*, 12(12), 7298–7312. <https://doi.org/10.21037/jtd-20-3339>
- Sharma, G. (2017). Color fundamentals for digital imaging. In *Digital Color Imaging Handbook* (pp. 1-114). CRC press.
- Sharma, V., Rathore, A., & Vyas, G. (2016). Detection of sickle cell anaemia and thalassaemia causing abnormalities in thin smear of human blood sample using image processing. In *2016 International Conference on Inventive Computation Technologies (ICICT)* (Vol. 3, pp. 1-5). IEEE Publishing. <https://doi.org/10.1109/inventive.2016.7830136>
- Shehab, M., Abualigah, L., Al Hamad, H., Alabool, H., Alshinwan, M., & Khasawneh, A. M. (2020). Moth-flame optimization algorithm: Variants and applications. *Neural Computing and Applications*, 32(14), 9859-9884. <https://doi.org/10.1007/s00521-019-04570-6>
- Shehanaz, S., Daniel, E., Guntur, S. R., & Satrasupalli, S. (2021). Optimum weighted multimodal medical image fusion using particle swarm optimization. *Optik*, 231, Article 166413. <http://dx.doi.org/10.1016/j.ijleo.2021.166413>
- Shi, M., Chen, C., Liu, L., Kuang, F., Zhao, D., & Chen, X. (2023). A grade-based search adaptive random slime mould optimizer for lupus nephritis image segmentation. *Computers in Biology and Medicine*, 160, Article 106950. <https://doi.org/10.1016/j.compbiomed.2023.106950>
- Singh, J., Kumar, V., Sinduja, K., Ekvitayavetchanukul, P., Agnihotri, A. K., & Imran, H. (2025). Enhancing heart disease diagnosis through particle swarm optimization and ensemble deep learning models. In *Nature-Inspired Optimization Algorithms for Cyber-Physical Systems* (pp. 313-330). IGI Global Scientific Publishing. <http://dx.doi.org/10.4018/979-8-3693-6834-3.ch010>
- Tavakoli, S., Ghaffari, A., Kouzehkanan, Z. M., & Hosseini, R. (2021). New segmentation and feature extraction algorithm for classification of white blood cells in peripheral smear images. *Scientific Reports*, 11(1), Article 19428. <https://doi.org/10.1038/s41598-021-98599-0>

- Tosta, T. A. A., De Abreu, A. F., Travencolo, B. A. N., do Nascimento, M. Z., & Neves, L. A. (2015). Unsupervised segmentation of leukocytes images using thresholding neighborhood valley-emphasis. In *2015 IEEE 28th International Symposium on Computer-Based Medical Systems* (pp. 93-94). IEEE Publishing. <https://doi.org/10.1109/cbms.2015.27>
- Vijh, S., Sharma, S., & Gaurav, P. (2020). Brain tumor segmentation using OTSU embedded adaptive particle swarm optimization method and convolutional neural network. In *Data Visualization and Knowledge Engineering: Spotting Data Points with Artificial Intelligence* (pp. 171-194). Springer International Publishing. http://dx.doi.org/10.1007/978-3-030-25797-2_8
- Wang, S., Cao, G., Wang, Y., Liao, S., Wang, Q., Shi, J., Li, C., & Shen, D. (2021). Review and prospect: Artificial intelligence in advanced medical imaging. *Frontiers in Radiology, 1*, Article 781868. <https://doi.org/10.3389/fradi.2021.781868>
- WHO. (2011). *Sickle Cell Disease and other Haemoglobin Disorders* [Fact Sheet No 308]. World Health Organization. <https://aho.org/fact-sheets/sickle-cell-disease-and-other-haemoglobin-disorders-fact-sheet/>
- Xu, M., Papageorgiou, D. P., Abidi, S. Z., Dao, M., Zhao, H., & Karniadakis, G. E. (2017). A deep convolutional neural network for classification of red blood cells in sickle cell anemia. *PLoS Computational Biology, 13*(10), Article e1005746. <https://doi.org/10.1371/journal.pcbi.1005746>
- Zhang, L., & Lim, C. P. (2020). Intelligent optic disc segmentation using improved particle swarm optimization and evolving ensemble models. *Applied Soft Computing, 92*, Article 106328. <https://doi.org/10.1016/j.asoc.2020.106328>
- Zhang, M., Li, X., Xu, M., & Li, Q. (2018). RBC semantic segmentation for sickle cell disease based on deformable U-Net. In *Medical Image Computing and Computer Assisted Intervention—MICCAI 2018: 21st International Conference* (pp. 695-702). Springer. https://doi.org/10.1007/978-3-030-00937-3_79
- Zhou, Z., & Liao, G. (2022). A novel approach to form normal distribution of medical image segmentation based on multiple doctors' annotations. In *Proceedings of SPIE--the International Society for Optical Engineering* (Vol. 12032). NIH Public Access. <https://doi.org/10.1117/12.2611973>